Atmospheric
Chemistry
and Physics

Open Access

Chemical composition and size distribution of summertime PM$_{2.5}$ at a high altitude remote location in the northeast of the Qinghai–Xizang (Tibet) Plateau: insights into aerosol sources and processing in free troposphere

J. Z. Xu[1]**, Q. Zhang**[2,3]**, Z. B. Wang**[1]**, G. M. Yu**[1]**, X. L. Ge**[2]**, and X. Qin**[1]

[1]Qilian Shan Station of Glaciology and Ecologic Environment, State Key Laboratory of Cryospheric Sciences,
Cold and Arid Regions Environmental and Engineering Research Institute, CAS, Lanzhou 730000, China
[2]Department of Environmental Toxicology, University of California, Davis, California 95616, USA
[3]Department of Environmental Science and Engineering, Fudan University, 220 Handan Road, Shanghai 200433, China

Correspondence to: J. Z. Xu (jzxu@lzb.ac.cn)

Abstract. Aerosol filter samples were collected at a high-elevation mountain observatory (4180 m a.s.l.) in the northeastern part of the Qinghai–Xizang (Tibet) Plateau (QXP) during summer 2012 using a low-volume sampler and a micro-orifice uniform deposit impactor (MOUDI). These samples were analyzed for water-soluble inorganic ions (WSIs), organic carbon (OC), elemental carbon (EC), water-soluble organic carbon (WSOC), and total organic nitrogen (TON) to elucidate the size-resolved chemical composition of free tropospheric aerosols in the QXP region. The average mass concentration of the sum of the analyzed species in PM$_{2.5}$ (particle matter) (WSIs + OC + EC + TON) was 3.74 μg sm^{-3}, 36 % of which was sulfate, 18 % OC, 17 % nitrate, 10 % ammonium, 6.6 % calcium, 6.4 % TON, 2.6 % EC, 1.5 % sodium, 0.9 % chloride, 0.5 % magnesium, and 0.3 % potassium. The size distributions of sulfate and ammonium peaked in the accumulation mode (0.32–0.56 μm), whereas the size distributions of both nitrate and calcium peaked in the range of 1.8–3.2 μm, suggesting the formation of nitrate on mineral dust. OC, EC and TON were also predominantly found in the accumulation mode. The bulk chemical composition and the average oxidation degree of water-soluble organic matter (WSOM) were assessed using a high-resolution time-of-flight aerosol mass spectrometer (HR-ToF-AMS). WSOM was found to be highly oxidized in all PM$_{2.5}$ samples with an average oxygen-to-carbon atomic ratio (O / C) of 1.16 and an organic mass-to-organic carbon ratio (OM / OC) of 2.75. The highly oxidized WSOM was likely related to active cloud processing during upslope air mass transport coupled with strongly oxidizing environments caused by snow/ice photochemistry. High average ratios of OC / EC (7.6) and WSOC / OC (0.79) suggested that organic aerosols were primarily made of secondary species. Secondary organic aerosol (SOA) was estimated on average accounting for 80 % (62–96 %) of the PM$_{2.5}$, indicating that SOA is an important component of free tropospheric aerosols over the northern QXP.

1 Introduction

The Qinghai–Xizang (Tibet) Plateau (QXP), often called "the third pole" (Yao et al., 2012), is one of the most remote and isolated regions in the world. The high altitude of this region has long been recognized as ideal for studying the long-range transported air pollutants. However, measurements from this area have been rare, usually due to the harsh natural conditions and logistic difficulties. These restrictions have become less problematic in the last decade because of the development of mountain observatories and improvements in sampling instrumentation (Li et al., 2000; Cong et al., 2007; Bonasoni et al., 2008; Hegde and Kawamura, 2012; Sang et al., 2013).

Previous studies in the QXP region have focused on the chemical properties of aerosols and their source signatures due to the important roles of aerosols on climate forcing. A few studies conducted at the Himalayas revealed that aerosols in this region are a complex mixture of inorganic and organic compounds (Carrico et al., 2003; Rengarajan et al., 2007; Decesari et al., 2010; Ram et al., 2010). Mineral dust was generally found to be an important constituent of aerosols in the QXP region because of the presence of large arid and semi-arid areas in "high Asia". A relatively large proportion of carbonaceous aerosols was also observed when the region was influenced by air masses transported from South Asia, where widespread usage of biofuels has led to large emissions of biomass burning aerosols (Engling et al., 2011; Zhao et al., 2013). Indeed, analysis of the chemical compositions of snow pit samples collected from a glacier in the central Himalayas indicated that biomass burning particles were significantly enhanced in snow during the winter–spring periods, due to transport of polluted air masses from northwest India and Nepal (Xu et al., 2013b).

Although inorganic species (such as mineral dust) are important aerosol components in the QXP, their chemical process in the atmosphere is reasonably well characterized due to the small number of inorganic species and their relatively simple chemistry. There have been increased interests in the organic constituents of aerosol particles in recent years because of their high abundances, complex chemical processing, and important roles in affecting cloud properties (e.g., Kanakidou et al., 2005; Jimenez et al., 2009). Organic aerosol (OA) is usually dominated by secondary species in remote regions (Zhang et al., 2007) because of atmospheric aging processes during long-range transport. For example, the average oxygen-to-carbon (O / C) atomic ratio, which is an indicator for the oxidation degree of OA, observed in a remote site in western Canada, was 0.83 (Sun et al., 2009), similar to the O / C ratios of highly aged, low-volatility (LV) oxygenated organic aerosol (OOA) in the atmosphere determined via positive matrix factorization (PMF) analysis of the aerosol mass spectrometer (AMS) spectra of OA (Ulbrich et al., 2009; Zhang et al., 2011). However, the extent of OA oxidation and the composition of organic species are closely related to the source characteristics, and the aging processes that are involved, which have never been carefully evaluated and determined in the QXP.

Most previous studies of aerosol chemistry in the QXP were conducted in the Himalayan regions because of the key roles of the Himalayas on regional climate and environment. There have been very few studies on aerosols reported from the northern QXP (Meng et al., 2013), despite the fact that their atmospheric behaviors might be significantly different from those found in the Himalayan regions because of the different climate pattern and aerosol sources in these two regions. For example, aerosols in the northern QXP mainly originate from inland China, whereas aerosols in the Himalayas mainly originate in India. Also, fine particles in the northern QXP tend to contain large proportions of sulfate (Xu et al., 2014a; Zhang et al., 2014b), while fine particles in the Himalayas are usually dominated by carbonaceous material.

The Qilian Shan Station of Glaciology and Ecologic Environment (QSS) is situated on the northern slope of the western Qilian Shan Mountains, in the northeastern part of the QXP (Fig. S1 in the Supplement). Due to its high elevation (4180 m a.s.l) and long distance (200 km) from local pollution sources, the QSS is well suited for sampling background air masses. In addition, the QSS is located near the termini of several glaciers, making this area a unique atmospheric environment where the photochemistry of snow and glaciers has a relatively strong effect.

In our previous studies, the seasonal variations of the mass concentration of water-soluble ions and the number concentration of particles at the QSS have been characterized (Xu et al., 2013a, 2014a), which presented two maxima in spring and summer. The first maximum corresponded to the period during which dust storms predominantly occur in North China, while the second peak corresponded to the period when the thermal circulation between areas of high and low elevation is strongest, where by the prevailing valley wind in the northeast of the QSS blew the polluted air masses to this region. In the present study, we performed an intensive field measurement study during the summer of 2012 with the aim of determining the chemical characteristics and sources of fine particles at the QSS during summer period. Here, we investigated the PM$_{2.5}$ (particle matter) chemical compositions and the properties of the associated organic chemical species, such as elemental ratios, by applying a suite of instruments including a high-resolution time-of-flight mass spectrometer (HR-ToF-AMS). The elemental ratios of organic species are valuable in understanding the oxidation state of OA and thus the aging processes that had occurred during its long-range transport. The size distributions of the chemical species were also assessed to understand the sources and chemical processes of aerosol.

2 Sample collection and analysis

2.1 Aerosol sampling

The samples were collected at the QSS atmospheric chemistry observatory (39.50° N, 96.51° E; 4180 m a.s.l.; Fig. S1). The sampling site and the QSS were described in detail by Xu et al. (2013a). The summer climate at the QSS is dominated by the East Asian monsoon, which brings about half of the annual precipitation (360 mm during 2008–2010). This study was conducted from 11 July to 6 September 2012. PM$_{2.5}$ samples were collected using a low-volume (16.7 L min^{-1} flow rate) aerosol sampler (BGI, USA, model PQ 200), powered by solar cells. The instrument was regularly calibrated using a TetraCal® calibrator (BGI, USA).

All samples were collected on 47 mm quartz fiber filters (Whatman, Maidstone, England). The flow rate was measured at 5 min intervals by an internal volume flow meter, and the recorded flow data were used to calculate the volume of air sampled. Meteorological parameters including wind speed, wind direction, temperature, precipitation, and relative humidity were recorded at 30 min intervals at the meteorological station at the QSS, and the recorded data were used to calculate the air volume sampled at standard temperature and pressure (STP; 1013 hPa and 273 K). Collection of each sample started in the morning and continued for 3 days, and a total of 19 aerosol filter samples were obtained. Three procedure blanks were collected in the field to assess potential contamination that could have occurred during sampling preparation, transportation, and storage. The sampling volume ranged from 42 to 44 m^3 under STP (i.e., sm^3), with a mean ($\pm 1\sigma$) value of 43.2 ± 0.5 sm^3. Note that the mass concentrations reported here are all based on STP (e.g., μg sm^{-3}).

In addition, measurements of the size distribution of chemical species were made at the QSS from 21 July to 4 September 2012. A 10-stage multi-nozzle micro-orifice uniform deposit impactor (MOUDI; Model R110, MSP Corp., Shoreview, MN) was used to sample particles at a flow rate of 30 L min^{-1} over a size range of 0.056–18 μm with nominal cut offsets of 0.056, 0.10, 0.18, 0.32, 0.56, 1.0, 1.8, 2.5, 5.6, 10, and 18 μm. The air pump was calibrated before each sample was collected and the pump was closely monitored to identify any changes of the flow rate. The collection substrates were 47 mm quartz fiber filters which had been heated at 500 °C for 8 h prior to sample collection to remove adsorbed organic material. The sampling time varied between $\sim$20 and $\sim$120 h depending on weather conditions. A total of four sets of filters were obtained. All the filters were placed in individual aluminum-lined plastic boxes and stored at -15 °C prior to analysis.

2.2 Chemical analysis

The samples were analyzed to characterize their chemical compositions using a series of instruments, namely ion chromatography (IC) instruments, a total water-soluble organic carbon / total nitrogen (TOC / TN) analyzer, a HR-ToF-AMS, and an organic carbon / element carbon (OC / EC) analyzer. For each OC / EC analysis, a piece of filter measuring at 0.526 cm^2 was punched from a sample filter and analyzed directly using the instrument. The rest of that filter was extracted by sonication in 15 mL deionized water for 30 min at $\sim$0 °C, and the extract was immediately filtered using a 0.45 μm Acrodisc syringe filter (Pall Life Sciences, Ann Arbor, MI, USA).

2.2.1 IC analysis

Eight ionic species (Na$^+$, NH$_4^+$, K$^+$, Ca^{2+}, Mg^{2+}, Cl$^-$, NO$_3^-$, and SO$_4^{2-}$) were determined using two IC systems (881 Compact IC Pro, Metrohm, Herisau, Switzerland). One of the IC systems was used to determine cations, and was equipped with a Metrosep C4 guard/2.0 column and Metrosep C4 250/2.0 column (Metrohm), which were kept at 30 °C during measurements. The other IC system, equipped with a Metrosep RP2 guard/3.6 column and a Metrosep A Supp15 250/4.0 column (Metrohm), and kept at 45 °C during measurements, was used to determine anions. The mobile phase in the cation IC system was 1.75 mM nitric acid (made from 70 % nitric acid, Sigma-Aldrich, St Louis, MO, USA) and 0.75 mM dipicolinic acid (made from $\geq$ 99.5 % pure dipicolinic acid, Sigma-Aldrich), and eluted at a flow rate of 0.3 mL min^{-1}. The eluent of anion IC system was 5 mM sodium carbonate and 0.3 mM sodium hydroxide (made from $\geq$ 98 % pure sodium hydroxide, Sigma-Aldrich), and was used at a flow rate of 0.8 mL min^{-1}. The instruments were calibrated using standard cation and anion solutions (Dionex, CA, USA). The IC analysis results were evaluated in terms of the reproducibilities of peak retention times, peak heights, and the linearity of each calibration curve. More details on the IC analysis methods are given in Ge et al. (2014).

2.2.2 TOC and TN analysis

An aliquot of each sample was analyzed for TOC and TN contents using a high-sensitivity TOC/TN analyzer (TOC-V$_{CPH}$ with a TNM-1unit, Shimadzu, Kyoto, Japan). The measurements were carried out using the total carbon (TC) and inorganic carbon method. The TC was determined by combusting the sample at 720 °C in a combustion tube filled with an oxidation catalyst, which converted all carbon-containing components into CO$_2$. The CO$_2$ was detected by a non-dispersive infrared (NDIR) gas analyzer. The inorganic carbon was defined as the carbon in carbonates and dissolved CO$_2$ in the sample. The carbonates were transformed into CO$_2$ by treating the sample with 25 % (by weight) phosphoric acid (H$_3$PO$_4$) in an inorganic carbon reaction vessel. The CO$_2$ was then volatilized using a sparging procedure and detected by the NDIR analyzer. The TOC content was calculated by subtracting the inorganic carbon content from TC content. In the TN analysis the nitrogen-containing species were decomposed to NO in the combustion tube at 720 °C, then the sample was cooled and dehumidified using an electronic dehumidifier, and the NO was measured using a chemiluminescence gas analyzer. The total organic nitrogen (TON) was determined by subtracting the inorganic nitrogen (which included ammonium and nitrate) content, quantified by IC, from the TN content. The samples were contained in well-sealed, pre-cleaned glass vials during analysis, and the instruments automatically withdrew a sample aliquot after piercing the vial seal. The calibrations were carried out us-

ing a potassium hydrogen phthalate standard for the TC determination, a sodium hydrogen carbonate for the inorganic carbon determination, and potassium hydrogen phthalate and potassium nitrate standards for the TN determination.

2.2.3 HR-ToF-AMS analysis

Each filtered sample extract was aerosolized using argon and dehumidified using a diffusion dryer. The resulting aerosol particles were sampled into a HR-ToF-AMS instrument (Aerodyne Inc., Billerica, MA, USA) through an aerodynamic lens inlet, vaporized at $\sim 600\,°C$, ionized by 70 eV electrons in an electron impact ionization chamber, and analyzed using the mass spectrometer. The HR-ToF-AMS analysis procedure for aqueous samples and associated data processing are described in detail elsewhere (Sun et al., 2010, 2011; Xu et al., 2013b; Yu et al., 2014). The HR-ToF-AMS was operated in the "V" and "W" ion optical modes alternatively, spending 2.5 min in each mode. In the V-mode the HR-ToF-AMS spent 6 s in the mass spectrum (MS) mode and then 4 s in the particle time-of-flight (PToF) mode, then continuously repeated this 10 s cycle. In the W-mode the instrument used only the MS mode, with 6 s in each cycle. Between every two samples, purified waters ($> 18.2\,\mathrm{M\,cm^{-1}}$, Millipore, USA) were analyzed in the same way to generate analytical blanks. Each sample was measured twice to check the reproducibility of the analysis. Elemental analyses were performed on high-resolution mass spectra (W-mode, with m/z up to 120), and these were used to determine the elemental ratios for oxygen to carbon (O / C), hydrogen to carbon (H / C), nitrogen to carbon (N / C), and organic mass-to-organic carbon (OM / OC) ratio of the water-soluble organic matter (WSOM) (Aiken et al., 2008). The elemental contributions of C, O, H, and N reported in this study are mass based. The signals of H_2O^+ and CO^+ for organic compounds were not directly measured but scaled to that of CO_2^+ based on the evaluation of the H_2O^+ and CO^+ signal in the samples (Fig. S3): $H_2O^+ = 0.94 \times CO_2^+$, $CO^+ = 0.46 \times CO_2^+$.

Potential interferences on the CO_2^+ signals in the aerosol mass spectra caused by the presence of carbonate salts were evaluated by acidifying a sample (QSS1) to pH 4 using sulfuric acid and then analyzing the sample using the HR-ToF-AMS. Meanwhile, the volatility of the sample was investigated by a digitally controlled thermodenuder (TD) system. The sample was aerosolized and passed through a diffusion dryer, switched between the by-pass (BP) mode and TD mode every 5 min, and finally analyzed using the HR-ToF-AMS instrument. The TD system was programmed to cycle through 12 temperature steps (30, 50, 70, 100, 150, 200, 180, 130, 110, 88, 66, and then $40\,°C$). The design and use of the TD system have been described elsewhere (Fierz et al., 2007). The data were processed in a similar way as the normal HR-ToF-AMS data analysis, and the remaining particle mass calculated from the difference between the results of

the TD mode and the BP mode analyses were assumed to indicate the volatility of individual aerosol species.

2.2.4 OC and EC analysis

The samples were analyzed for OC / EC using a Thermal/Optical Carbon Analyzer (DRI Model 2001). The procedure used has been described in detail elsewhere (Cao et al., 2003). Briefly, the system heated the $0.526\,\mathrm{cm}^2$ punched quartz filter aliquot gradually to $120\,°C$ (fraction OC1), $250\,°C$ (fraction OC2), $450\,°C$ (fraction OC3), and $550\,°C$ (fraction OC4) in a non-oxidizing helium atmosphere, and then to $550\,°C$ (fraction EC1), $700\,°C$ (fraction EC2), and $800\,°C$ (fraction EC3) in an oxidizing atmosphere of 2 % oxygen in helium. The carbon evolved at each temperature was oxidized to CO_2, then reduced to methane (CH_4) and quantified using a flame ionization detector. Some of the organic carbon was pyrolyzed to form black carbon as temperature increased in the helium atmosphere, resulting in the darkening of the filter. This darkening was monitored by measuring the decrease in the reflectance of the sample using light at 633 nm from a He–Ne laser. The original black carbon and the pyrolyzed black carbon combusted after being exposed to the oxygen-containing atmosphere, and the reflectance increased. The amount of carbon measured after exposure to the oxygen-containing atmosphere until the reflectance reached its original value was reported as the optically detected pyrolyzed carbon (OPC). The eight fractions, OC1, OC2, OC3, OC4, EC1, EC2, EC3, and OPC, were reported separately. OC was defined as OC1 + OC2 + OC3 + OC4 + OPC and EC was defined as EC1 + EC2 + EC3 − OPC in the IMPROVE (Interagency Monitoring of Protected Visual Environments) protocol.

2.2.5 Determination of the WSOM and water-insoluble organic mass concentrations

The mass concentrations of WSOM and water-insoluble OM (WIOM), and the average OM / OC ratio for the organic matter (WSOM + WIOM) in PM$_{2.5}$ are estimated using Eqs. (1)–(3)

$$\mathrm{WSOM} = \mathrm{WSOC} \times \mathrm{OM} / \mathrm{OC_{WSOM}}, \qquad (1)$$

$$\mathrm{WIOM} = (\mathrm{OC} - \mathrm{WSOC}) \times 1.3, \qquad (2)$$

$$\mathrm{OM} / \mathrm{OC_{OM}} = (\mathrm{WSOM} + \mathrm{WIOM}) / \mathrm{OC}, \qquad (3)$$

where WSOC is the water-soluble organic carbon content in the filter extract measured by the TOC / TN analyzer, OM / OC$_{\mathrm{WSOM}}$ is the OM / OC ratio of the WSOM (determined from the HR-ToF-AMS measurement), OC is taken from the filter measurements using the thermo-/optical carbon analyzer, the constant 1.3 in Eq. (2) is the estimated OM / OC for WIOM (Sun et al., 2011), and OM / OC$_{\mathrm{OM}}$ is the average OM / OC ratio of organic matter in PM$_{2.5}$.
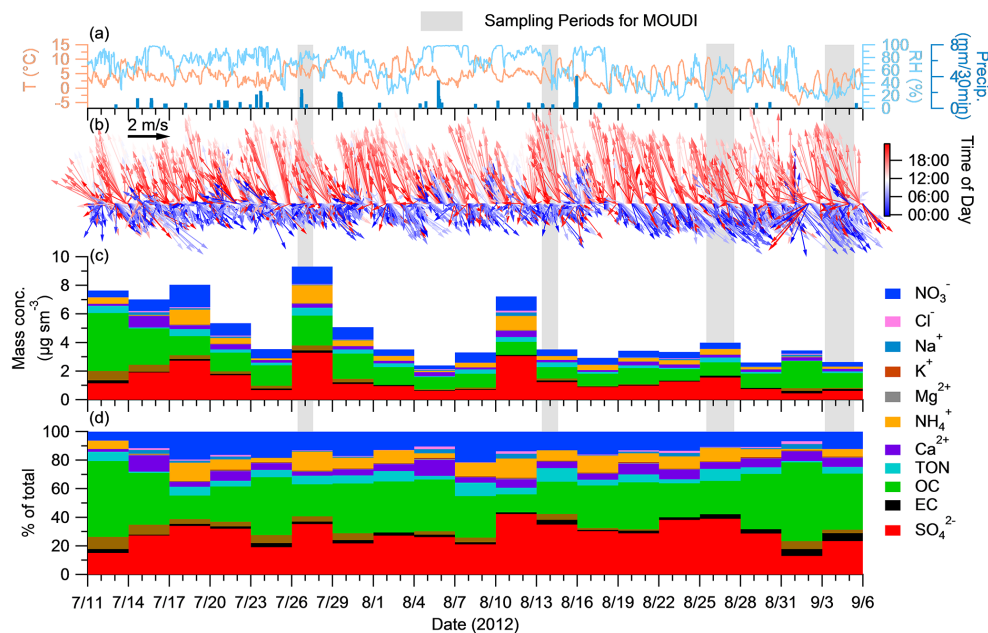
Figure 1. Time series of **(a)** meteorological data, **(b)** wind speed and wind direction colored by time of day (Beijing Time), **(c)** mass concentrations of water-soluble ions, organic carbon (OC), elemental carbon (EC), and total organic nitrogen (TON) in PM$_{2.5}$, and **(d)** percent contributions of various species to total mass.

2.2.6 Estimation of the secondary organic aerosol concentrations

The secondary organic carbon (SOC) content was estimated by determining the primary organic carbon (POC) content using EC as a tracer, and then subtracting the POC from the measured total OC. The primary OA (POA) concentration was estimated based on POC, which was subtracted from the total OM calculated as the product of the measured OC, and the OM / OC$_{OM}$ determined in Eq. (3) to determine the secondary OA (SOA) concentration. The equations for these calculations are shown below:

$$POC = (OC / EC)_{pri} \times EC, \tag{4}$$

$$SOC = OC - POC, \tag{5}$$

$$POA = OM / OC_{POA} \times POC, \tag{6}$$

$$SOA = OC \times OM / OC_{OM} - POA. \tag{7}$$

The calculation of POC was based on the hypothesis that OC and EC correlate strongly and stay at a constant ratio in primary particles within a geographical region. Organic aerosol observed at the QSS mostly originated from lower attitude regions including an urban area east and west of the QSS based on the typical diurnal pattern of the wind field around the QSS (Xu et al., 2014a). Based on previous studies, the OM / OC for fresh urban organics in northern China is between 1.2 and 1.6 (e.g., Xu et al., 2014b; Zhang et al., 2014a). Since it is expected that organics would be oxidized gradually during transport, we use the ratio of 1.4 for OM / OC of the POA (OM / OC$_{POA}$) at the QSS.

3 Results and discussion

3.1 Chemical speciation of PM$_{2.5}$

The meteorological conditions during the measurement period were overall cold and humid. The air temperature (T) ranged from −5.9 to 14.3 °C, with an average of 4.2 °C, and the relative humidity (RH) ranged from 10 to 99 %, with an average of 65 % (Fig. 1a); 3-day air mass back trajectories originating at ∼ 100 m a.g.l. were acquired every 6 h during the sampling period and showed that 72 and 23 % of the air masses came from west and east of the sampling site, respectively (Fig. S1). Light precipitation occurred frequently between 11 July and 19 August (Fig. 1a) because of the topographic effect, but it was relatively dry from 19 August to 6 September, probably because of the occurrence of a different synoptic-scale weather pattern. The 3-day average wind data also showed that the wind speed from west increased during the late part of the sampling period (Fig. S2). Wind direction changed diurnally, with moderate mountain wind (from the southeast at ∼ 2 m s^{-1}) during the night and stronger valley wind (from the north at ∼ 4 m s^{-1}) during the day (Fig. 1b). The concentrations of various chemical species, including water-soluble ionic species (WSIs), OC, EC, and TON, changed significantly according to weather condition throughout the sampling period. No dust storm event was observed during the study even though the QSS is close to the desert regions.

The total mass concentrations of the measured species (WSIs + OC + EC + TON) throughout the sampling pe-
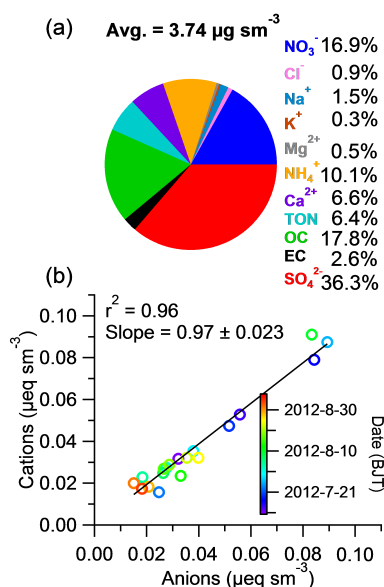
Figure 2. (a) The average composition of the species analyzed and (b) the charge balance between the cations ($Na^+ + NH_4^+ + K^+ + Mg^{2+} + Ca^{2+}$) and anions ($Cl^- + SO_4^{2-} + NO_3^-$).

riod were in the range of 1.8–8.0 µg sm^{-3} with the average ($\pm 1\sigma$) at 3.7 $\pm$ 1.9 µg sm^{-3} (Fig. 2a), which were lower than that was measured in 2010 (2.7 µg sm^{-3} in 2012 vs. 5.4 µg sm^{-3} in 2010 for the same WSIs in July and August) at the QSS (Xu et al., 2014a), probably because of the low frequency of dust storm events in 2012. Indeed, mass concentration of calcium was more than 4 times lower in 2012 (0.27 µg sm^{-3}) than that in 2010 (1.2 µg sm^{-3}). Overall, sulfate was the main contributor (on average 36 %) to the aerosol mass concentrations during the observation period (Fig. 2a), similar to previous observations in the northern QXP (Li et al., 2013; Xu et al., 2014a; Zhang et al., 2014b). The mass concentration of sulfate was also lower in 2012 (1.4 µg sm^{-3}) than that in 2010 (2.7 µg sm^{-3}). Major cations – ammonium (10 %), calcium (6.6 %), sodium (1.5 %), magnesium (0.5 %), and potassium (0.3 %) – and anions – sulfate (36.2 %), nitrate (16.9 %), chloride (0.9 %) – together accounted for 45–88 % (mean = 73 %) of the total aerosol mass. The ion balance, expressed as the ratio of the equivalent concentration (µeq sm^{-3}) cation to that of anion (C / A), is shown in Fig. 2b. The mean C / A ratio was 0.97, which was close to 1, further indicating that the contribution of mineral dust was negligible since carbonate and bicarbonate were not measured in the IC analyses. The average EC concentration was 0.09 µg sm^{-3} during the observation period, and its mean contribution to the total PM$_{2.5}$ mass was 2.6 %. The average ($\pm 1\sigma$) concentrations of OC and TON were 0.66 ($\pm$0.43) and 0.24 ($\pm$0.16) µg sm^{-3}, respectively. The OC and EC concentrations found in this study were lower than those found in the summer of 2010 at Qing-

hai Lake (1.6 and 0.4 µg sm^{-3}), which is also in the northern part of the QXP. The concentrations were different probably because Qinghai Lake is located at a lower elevation (3200 m a.s.l.; Li et al., 2013) than the QSS (4180 m a.s.l.) and is subjected to more emissions from the boundary layer.

The correlation coefficients (r) between all of the chemical species are shown in Table 1, and the strong correlations ($r \geq 0.75$) are shown in bold. In general, strong correlations were found between Na$^+$ and Ca^{2+}, Mg^{2+}, and Cl$^-$, which are representative of primary species in mineral salts, and among secondary ions such as SO$_4^{2-}$, NO$_3^-$, and NH$_4^+$. In addition, the good correlations between secondary ions (SO$_4^{2-}$ and NO$_3^-$) and K$^+$ and Mg^{2+} might arise from acid replacement on mineral particles. The facts that WSOC and OC tightly correlate ($r = 0.97$) and that WSOC accounts for 79 % of the OC indicate that a majority of OC in fine particles was secondary at the QSS (more discussions are given in Sect. 3.3).

3.2　Chemically resolved size distributions

The size distributions of all species are shown in Fig. 3, and the sum of the species presents a prominent accumulation mode peaking at a MOUDI stage of 0.32–0.56 µm and a coarse mode peaking at 1.8–3.2 µm. In the accumulation mode, sulfate dominated (39 %) the composition of particles in the size range of 0.18–1 µm, with OC and EC accounting for 24 % and 5.0 %, respectively, followed by TON (9.4 %), NH$_4^+$ (7.9 %), NO$_3^-$ (3.9 %), Cl$^-$ (2.8 %), K$^+$ (1.3 %), and Ca^{2+} (0.6 %). However, OC dominated (36 %) the composition of particles smaller than 0.18 µm with sulfate contributing 26 %. In the coarse mode, nitrate was the main contributor, accounting for 23 % of the particle mass in the size range 1.8–5.6 µm, followed by OC (17 %), sulfate (16 %), TON (12 %), Ca^{2+} (11 %), Cl$^-$ (8.4 %), and EC (2.2 %); the rest of the species in total accounted for 3.7 % at this size range. TON and OC were important contributors of particle mass over the whole size range (0.056–18 µm).

The different size distributions of different species suggested that they had different sources and/or have undergone atmospheric transformation processes. The species that were relatively abundant in the accumulation mode aerosols were mainly secondary species, such as ammonium, sulfate, and OC, while the species that were relatively abundant in the coarse mode aerosols were mainly primary mineral ionic species, such as Ca^{2+}, Na$^+$, and Cl$^-$. Nitrate was closely associated with dust particles as a result of its formation through the reactions of HNO$_3$ gas with carbonate salts (such as calcite and dolomite) (Sullivan et al., 2009) which could form Ca(NO$_3$)$_2$ and Mg(NO$_3$)$_2$ (Li and Shao, 2009). As shown in Fig. 4, the equivalent balances of water-soluble species in different size modes indicate that the accumulation mode particles were somewhat acidic (with the linear regression slope of [NH$_4^+$ + Ca^{2+} + Mg$^+$ + K$^+$] vs. [SO$_4^{2-}$ + NO$_3^-$] being 0.6) and that the coarse mode particles were al-

Table 1. Correlation coefficients (Pearson's r) between the water-soluble inorganic ions, organic carbon (OC), elemental carbon (EC), water-soluble organic carbon (WSOC), and total organic nitrogen (TON) concentrations ($n = 19$). Values that indicate a strong correlation (i.e., $r \geq 0.75$) are in bold.

	Na$^+$	NH$_4^+$	K$^+$	Mg^{2+}	Ca^{2+}	Cl$^-$	SO$_4^{2-}$	NO$_3^-$	EC	WSOC	OC
NH$_4^+$	0.28										
K$^+$	0.38	**0.87**									
Mg^{2+}	**0.84**	0.51	0.63								
Ca^{2+}	**0.80**	0.04	0.23	**0.79**							
Cl$^-$	**0.85**	0.32	0.41	**0.83**	0.77						
SO$_4^{2-}$	0.57	**0.88**	**0.86**	**0.77**	0.47	0.58					
NO$_3^-$	0.41	**0.81**	**0.77**	0.67	0.35	0.42	**0.83**				
EC	-0.22	0.23	0.22	-0.26	-0.28	-0.22	0.10	0.03			
WSOC	-0.04	0.17	0.12	-0.10	0.10	-0.03	0.16	0.17	0.59		
OC	-0.01	0.16	0.14	-0.05	0.17	-0.01	0.18	0.23	0.56	**0.97**	
TON	-0.10	**0.81**	0.61	0.16	-0.16	-0.08	0.65	0.67	0.51	0.45	0.43

Figure 3. (a) Average size distributions of the mass concentrations of water-soluble inorganic ions (SO$_4^{2-}$, NO$_3^-$, Cl$^-$, NH$_4^+$, Ca^{2+}, Mg^{2+}, and K$^+$), total organic nitrogen (TON), elemental carbon (EC), and organic carbon (OC). **(b)** The fractional contributions of individual species to total mass in different size bins.

Figure 4. (a) Average equivalent concentrations water-soluble inorganic species in individual size bins. The vertical dashed line indicates the boundary between the accumulation mode and the coarse mode. **(b)** Scatter plot that compares the equivalent concentrations of cations (i.e., NH$_4^+$ + Ca^{2+}+ Mg^{2+}+ K$^+$) and the equivalent concentrations of anions (i.e., SO$_4^{2-}$+ NO$_3^-$) in the accumulation mode and coarse mode particles, respectively.

sites, e.g., Hong Kong, where the accumulation mode was at 1–1.8 μm and the coarse mode was at 3.2–5.6 μm (Xue et al., 2014). The smaller mode size at the QSS was probably because of the lower specific humidity at the QSS.

The OC and TON species in the coarse mode probably came from soil organic matter or were formed by the condensation of volatile organic gases on mineral dust. The EC and OC species reaching maximum concentrations in the accumulation mode, consistent with other results, indicating the occurrence of aging and aqueous processing of particles (Yu and Yu, 2009).

3.3 Relationship between OC, EC, and WSOC

The relationship between OC and EC concentrations can provide useful insights into the origin of carbonaceous aerosols, because particles from different sources have different OC / EC ratios. The correlation between EC and OC concentrations at the QSS was statistically significant ($r^2 = 0.4$,

most neutral (the slope was 0.999), similar to the results observed at Mount Hua in 2009 (Wang et al., 2013). The sizes of WSIs in this study were smaller than that observed at other
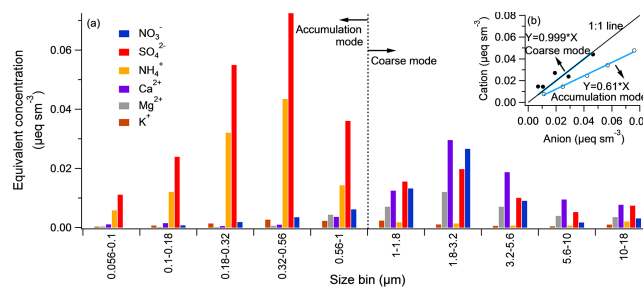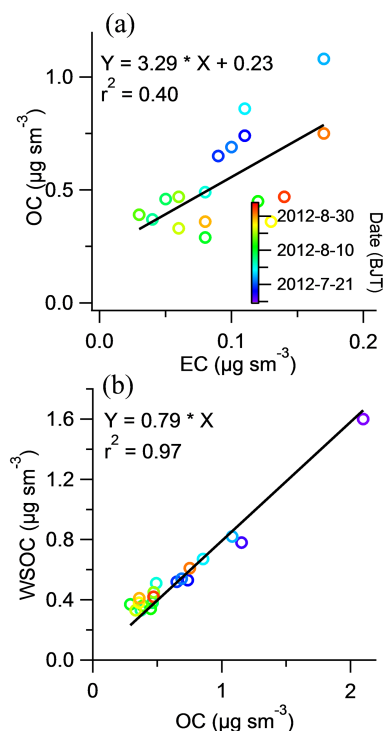
Figure 5. Scatter plots of **(a)** the organic carbon (OC) concentration against the elemental carbon (EC) concentration and **(b)** the water-soluble organic carbon concentration (WSOC) against the OC colored by the sampling date.

Figure 6. Average water-soluble organic carbon (WSOM) mass spectrum and mass concentration fraction (pie charts) colored by the contributions of six ion categories and elements (C, O, H, and N) for PM$_{2.5}$ filter samples.

$n = 19$), with the slope of 3.29 and the intercept of 0.23 (Fig. 5a and b). The OC / EC ratios ranged from 2.8 to 26.4 with an average of 7.6, which is higher than those observed from Chinese urban sites (1 to 4) (Cao et al., 2003). However, the OC / EC ratio at the QSS was similar to the ratios found at remote sites in western China (Fig. S1) such as Qinghai Lake (6.0 ± 3.9 in PM$_{2.5}$) during the summer of 2010 (Li et al., 2013), Muztagh Ata mountains (11.9 in total suspended particles) during the summers of 2004–2005 (Cao et al., 2009), and Akdala (12.2 in PM$_{10}$) during July 2004 and March 2005 (Qu et al., 2009). The high OC / EC ratios observed at the QSS suggest the formation of secondary OC during the long-range transport. The chemical characteristics of particulate organics can be further evaluated using the WSOC / OC ratio, which can be used to assess the aging of organic species. High WSOC / OC ratios (> 0.4) have been found in aged aerosols because a significant portion of the OC can be oxidized to WSOC (Ram et al., 2010). A tight correlation between WSOC and OOA was observed previously in Tokyo, indicating that OOA and WSOC have very similar chemical characteristics (Kondo et al., 2007). Field studies have shown that the OOA factors derived from multivariate analysis AMS organic aerosol mass spectra are generally representative of SOA (Zhang et al., 2005, 2011). The WSOC and OC concentrations in the QSS were strongly positively correlated
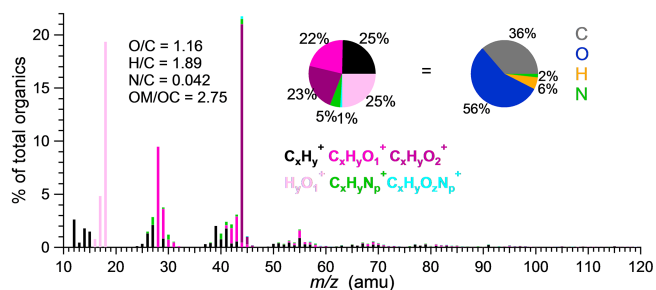
($r^2 = 0.97$) with a slope of 0.79. This slope is higher than those in Chinese urban sites (0.3–0.6) (Pathak et al., 2011) and at remote sites in western China, such as Qinghai Lake (0.42) during the summer of 2012 (Li et al., 2013) and the Himalayas (0.26–0.51) (Rengarajan et al., 2007; Ram et al., 2010; Shrestha et al., 2010). However, it is similar to the average ($\pm 1\sigma$) ratio of WSOC to OOA (0.88 ± 0.29) in Tokyo (Kondo et al., 2007). The high OC / EC ratios, tight WSOC and OC correlation, and the high WSOC / OC ratios found in the aerosol particles from the QSS can be regarded as a solid evidence for the formation of SOA in the QXP region.

3.4 Spectra characteristics of the WSOM

The average MS for the WSOM in PM$_{2.5}$ is shown in Fig. 6. The major spectral features are the high mass fraction of m/z 44 (f44) (mainly CO$_2^+$, 94.6 %), m/z 18 (H$_2$O$^+$), and m/z 28 (CO$^+$). The f44 peaks were almost identical (~ 20 %) in all filter samples, and in two samples, QSS3 and QSS18, the contributions of f44 peaks were particularly high, at 27.4 and 27.3 %, respectively. It has previously been suggested that CO$_2^+$ ion in the HR-ToF-AMS MS is typically associated with the presence of carboxylic acids (Takegawa et al., 2007), which can be the oxidation products of organic species through heterogeneous and homogeneous chemical processes (fragmentation) (Jimenez et al., 2009). This can be supported by the low intensity fragments in the higher m/z range ($m/z > 50$), which were probably caused by the fragmentation of organic species during oxidation and conversion into small organic acids (increased f44). The similarities between the mass spectra of the acidified and untreated QSS1 sample ($r^2 = 0.98$; Fig. S4) ruled out the potential influence of carbonate salts on the intensity of the CO$_2^+$ peak. The O / C ratio, an oxidation degree index, has a mean value of 1.16 and a range of 0.93–1.66 (Fig. 6a). The mean OM / OC ratio of WSOM in our filter samples was 2.75, which contrasts strongly with the range of 1.6–2.2 found in other studies, indicating that secondary organic aerosol made important contributions to the aerosols in our study. The H / C ratio was also relatively high, at 1.89.

The high O / C and H / C ratios were caused not only by the high contribution of CO_2^+ ions but also by the high contribution from H_2O^+, which can be produced by the fragmentation of acidic species. Carbon oxidation state (OSc) values are more robust and less variable than measured H / C and O / C ratios, so we calculated the OSc values ($2 \times$ O / C– H / C). The mean OSc for the filter samples was 0.4 ranging between 0.1 and 1.2, similar to the OSc values of diacids and multi-functional acids (Canagaratna et al., 2015). The elemental composition of the WSOM in the filter samples was C (36 %), O (56 %), H (6 %), and N (2 %). The mass spectrum was composed of $H_yO_1^+$ (25 %), $C_xH_yO_1^+$ (22 %), $C_xH_yO_2^+$ (23 %), and $C_xH_y^+$ (25 %) ions, indicating that oxygenated functional groups were predominant in the WSOM. The high contribution from $H_yO_1^+$ ions could be generated from diacids and alcohols (Canagaratna et al., 2015).

The high oxidation state of organics at the remote area of the northern QXP has been suggested in a previous study at Qinghai Lake in 2010 (Li et al., 2013). We sought further evidence for the high oxidation state of organics in our samples by checking the volatility of OC, which normally has a reverse relationship with the degree of oxidation (Huffman et al., 2009). The OC mass fractions that evaporated at different temperature steps were 12 % at 120 °C (OC1), 26 % at 250 °C (OC2), 39 % at 450 °C (OC3), and 23 % at 550 °C (OC4). The large fractions of OC at high temperature suggested its low volatility. Indeed, the volatility measurements performed using the TD system on the QSS1 sample indicated that the organic species were less volatile than ammonium and nitrate and more volatile than sulfate (Fig. 7a). However, the remaining fraction of organics was higher than sulfate at 180–200 °C (Fig. 7b). The volatility distribution of the WSOM of the QSS1 sample was similar to that of LV-OOA in samples from urban sites (Huffman et al., 2009). Note that the thermal profile of sulfate in our sample is similar to that of ammonium sulfate but nitrate appears to be less volatile than ammonium nitrate based on the laboratory study of Huffman et al. (2009); a possible reason is that the nitrate in filter aerosol was mainly present in the form or organic nitrate or metal nitrate. The ratio of NO^+ vs. NO_2^+ in mass spectrum of the QSS filter samples indeed shows higher values than that of ammonium nitrate which usually resulted from the organic nitrate or metal nitrate (Farmer et al., 2010) (Fig. S6). This is consistent with the fact that a significant fraction of nitrate in these samples was likely associated with metals such as calcium and sodium (Fig. 2).

The AMS spectra showed that organic species in PM$_{2.5}$ collected at the QSS were on average more oxidized than low-volatility oxygenated organic aerosol factors (e.g., LV-OOA, which had an O / C ratio of 0.5–1) determined using PMF analyses of urban aerosols (Aiken et al., 2008; Ng et al., 2010). The higher level of oxidation of organic species in our samples was probably caused by intense photo-chemistry because of the stronger solar radiation in free troposphere
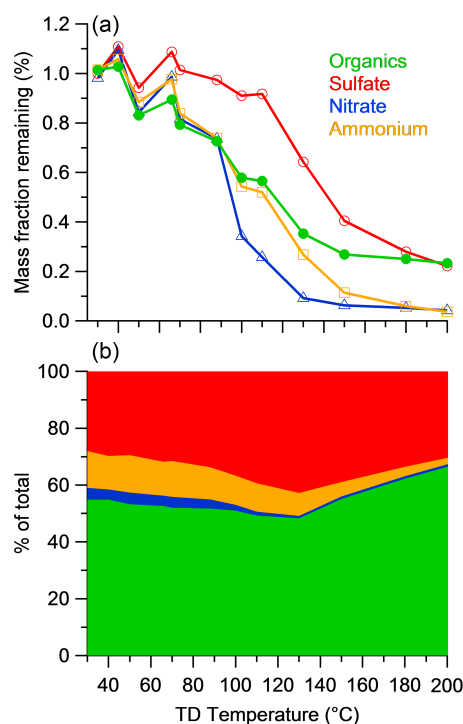

Figure 7. Thermal profiles of organic aerosol, sulfate, nitrate, and ammonium in PM$_{2.5}$ from the QSS based on **(a)** the mass fraction of remaining aerosol compared to ambient temperature; **(b)** the composition of non-refractory aerosol materials at given TD temperatures.

and/or aqueous-phase reactions in cloud droplets and particulate water phase during the upslope transport of air mass from the lowlands. Indeed, the highly oxidized organic MS observed in this study is similar to that of oxidized organic matter reported in the study of Lee et al. (2012) ($r^2 = 0.95$; Fig. S5), during which filter samples collected at a mountain site were oxidized in the laboratory using a photochemical reactor. The potentially strong oxidizing environment at the QSS was another important factor in producing the highly oxidized organic species. For example, the photochemical reactions on snow/ice are suspected to have released reactive gaseous species, including H_2O_2, HONO, and OH (Grannas et al., 2007).

3.5 Estimation of secondary organic aerosol concentrations

The EC-tracer method, which estimates SOC concentration based on the relationship of POC and EC, has been widely used, although significant uncertainty may arise due to the usage of assumed (OC / EC)$_{primary}$ ratios. In this study, a value of 2.0 is used to represent the (OC / EC)$_{primary}$ ratio at the QSS, which is commonly used to estimate SOA mass (Chow et al., 1996). In addition, this value is similar to the minimum OC / EC ratios that have been used for estimation
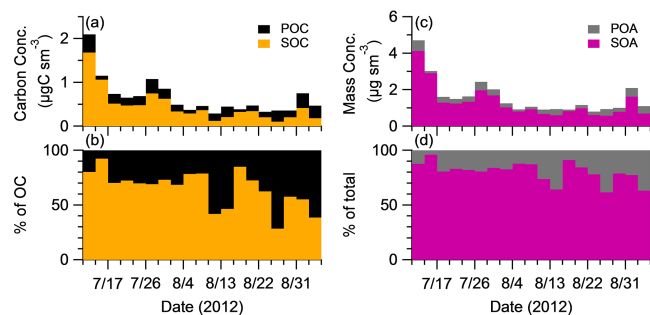
Figure 8. (a) and **(b)** estimated concentrations of primary and secondary organic carbon and their percent contributions to total OC in PM$_{2.5}$ from the QSS; **(c)** and **(d)** estimated primary and secondary organic aerosol mass concentrations and percent contributions to total OA mass.

of SOA concentration at remote sites in China, such as Mount Heng (2.2) (Zhou et al., 2012) and Mount Tai (2.19) (Wang et al., 2012). The minimum OC / EC (2.8) in the PM$_{2.5}$ samples at the QSS is higher than this value, which suggests the filter samples were likely always a mixture of POA and SOA due to the fact that each filter was collected for 3 days.

The average concentration of SOC at the QSS during the summer was $0.44 \pm 0.37 \, \mu g \, sm^{-3}$, on average accounting for 64 % (29–92 %) of the total OC (Fig. 8a and b). The average concentration of SOA was $1.27 \pm 0.88 \, \mu g \, sm^{-3}$, on average accounting for 80 % (62–96 %) of the total OA (Fig. 8c and d). These results indicate that secondary aerosols were dominant at the QSS during the summer. The SOC and SOA contributed relatively little to PM$_{2.5}$ mass during the late sampling period, and this is consistent with drier condition and thus fewer chances of aqueous processing during this period. The SOC contribution at the QSS is consistent with those (36–52 %) at the Himalayas during summer. For example, Ram et al. (2008) found, using the EC-tracer method, that SOC contributed 52 % of the aerosols at Manora Peak during summer. The estimated SOC contribution is also consistent with the results at Mount Heng (54 % of the total OC) and at Mount Tai (57 and 71 % of total OC in spring and summer, respectively) (Wang et al., 2012; Zhou et al., 2012).

4 Conclusions

An intensive study was conducted at a high elevation remote site (QSS) in the northern part of the QXP to characterize the chemical compositions of PM$_{2.5}$ during the summer of 2012 – a period that was influenced by a strong exchange of air masses between boundary layer and free troposphere. The average $\pm 1\sigma$ mass concentration of PM$_{2.5}$ species, which include WSIs (SO$_4^{2-}$, NO$_3^-$, NH$_4^+$, Ca^{2+}, Na$^+$, Cl$^-$, Mg^{2+}, and K$^+$), OC, EC, and TON, was $3.7 \pm 1.9 \, \mu g \, sm^{-3}$. Mineral dust appeared to be a minor PM$_{2.5}$ component during this study. SO$_4^{2-}$ was a main contributor to the PM$_{2.5}$ mass

(36 %), followed by OC (18 %), NO$_3^-$ (17 %), NH$_4^+$ (10 %), Ca^{2+} (6.6 %), TON (6.4 %), and EC (2.6 %). The size distribution of the particles presented a bimodal distribution with a prominent accumulation mode (0.32–0.56 μm) and a coarse mode (1.8–3.2 μm). Sulfate, OC, and EC dominated the accumulation mode (contributing ~ 70 % of the mass), while nitrate was a main contributor to the coarse mode (contributing 23 %), followed by OC (17 %), sulfate (16 %), TON (12 %), Ca^{2+} (11 %), Cl$^-$ (8.4 %), and EC (2.2 %). Stoichiometry analysis indicated that submicrometer particles were on average acidic, whereas coarse particles were mostly neutral. The facts that OC / EC ratios were high (2.8–26.4) and that a major fraction of OC was water soluble (79 %) suggest an important contribution of secondary OC to PM$_{2.5}$ composition at the QSS. Indeed, chemical characterization using HR-ToF-AMS showed that WSOM was mainly composed of highly oxygenated organic species. For example, the average AMS spectrum of WSOM was dominated by H$_y$O$_1^+$ (24 %), C$_x$H$_y$O$_1^+$ (22 %), C$_x$H$_y$O$_2^+$ (22 %), and C$_x$H$_y^+$ (26 %) ions and its O / C and OM / OC ratios were 1.16 and 2.75, respectively. These results suggest that organic species became highly oxidized during long-range transport from lowland to elevated mountain areas and/or locally in the northeastern region of QXP through intense photochemical and aqueous-phase processing in the free troposphere. The estimated SOA on average accounted for 80 % (range 62–96 %) of the PM$_{2.5}$ mass, which is higher than those reported from the Himalayas previously. Given that dry and wet deposition of aerosol particles strongly influences the chemical composition of snow and glaciers, our results may shed lights on the coupling between atmospheric chemistry and cryospheric chemistry in the northern QXP region.

The Supplement related to this article is available online at doi:10.5194/acp-15-5069-2015-supplement.

References

Aiken, A. C., DeCarlo, P. F., Kroll, J. H., Worsnop, D. R., Huffman, J. A., Docherty, K. S., Ulbrich, I. M., Mohr, C., Kimmel, J. R., Sueper, D., Sun, Y., Zhang, Q., Trimborn, A., Northway, M., Ziemann, P. J., Canagaratna, M. R., Onasch, T. B., Alfarra, M. R., Prevot, A. S. H., Dommen, J., Duplissy, J., Metzger, A., Baltensperger, U., and Jimenez, J. L.: O / C and OM / OC ratios of primary, secondary, and ambient organic aerosols with high-resolution time-of-flight aerosol mass spectrometry, Environ. Sci. Technol., 42, 4478–4485, doi:10.1021/es703009q, 2008.

Bonasoni, P., Laj, P., Angelini, F., Arduini, J., Bonafè, U., Calzolari, F., Cristofanelli, P., Decesari, S., Facchini, M. C., Fuzzi, S., Gobbi, G. P., Maione, M., Marinoni, A., Petzold, A., Roccato, F., Roger, J. C., Sellegri, K., Sprenger, M., Venzac, H., Verza, G. P., Villani, P., and Vuillermoz, E.: The abc-pyramid atmospheric research observatory in himalaya for aerosol, ozone and halocarbon measurements, Sci. Total. Environ., 391, 252–261, doi:10.1016/j.scitotenv.2007.10.024, 2008.

Canagaratna, M. R., Jimenez, J. L., Kroll, J. H., Chen, Q., Kessler, S. H., Massoli, P., Hildebrandt Ruiz, L., Fortner, E., Williams, L. R., Wilson, K. R., Surratt, J. D., Donahue, N. M., Jayne, J. T., and Worsnop, D. R.: Elemental ratio measurements of organic compounds using aerosol mass spectrometry: characterization, improved calibration, and implications, Atmos. Chem. Phys., 15, 253–272, doi:10.5194/acp-15-253-2015, 2015.

Cao, J. J., Lee, S. C., Ho, K. F., Zhang, X. Y., Zou, S. C., Fung, K., Chow, J. C., and Watson, J. G.: Characteristics of carbonaceous aerosol in pearl river delta region, china during 2001 winter period, Atmos. Environ., 37, 1451–1460, doi:10.1016/S1352-2310(02)01002-6, 2003.

Cao, J. J., Xu, B. Q., He, J. Q., Liu, X. Q., Han, Y. M., Wang, G. H., and Zhu, C. S.: Concentrations, seasonal variations, and transport of carbonaceous aerosols at a remote mountainous region in western china, Atmos. Environ., 43, 4444–4452, doi:10.1016/j.atmosenv.2009.06.023, 2009.

Carrico, C. M., Bergin, M. H., Shrestha, A. B., Dibb, J. E., Gomes, L., and Harris, J. M.: The importance of carbon and mineral dust to seasonal aerosol properties in the nepal himalaya, Atmos. Environ., 37, 2811–2824, doi:10.1016/s1352-2310(03)00197-3, 2003.

Chow, J. C., Watson, J. G., Lu, Z., Lowenthal, D. H., Frazier, C. A., Solomon, P. A., Thuillier, R. H., and Magliano, K.: Descriptive analysis of pm2.5 and pm10 at regionally representative locations during sjvaqs/auspex, Atmos. Environ., 30, 2079–2112, doi:10.1016/1352-2310(95)00402-5, 1996.

Cong, Z., Kang, S., Liu, X., and Wang, G.: Elemental composition of aerosol in the nam co region, tibetan plateau, during summer monsoon season, Atmos. Environ., 41, 1180–1187, doi:10.1016/j.atmosenv.2006.09.046, 2007.

Decesari, S., Facchini, M. C., Carbone, C., Giulianelli, L., Rinaldi, M., Finessi, E., Fuzzi, S., Marinoni, A., Cristofanelli, P., Duchi, R., Bonasoni, P., Vuillermoz, E., Cozic, J., Jaffrezo, J. L., and Laj, P.: Chemical composition of PM$_{10}$ and PM$_1$ at the high-altitude Himalayan station Nepal Climate Observatory-Pyramid (NCO-P) (5079 m a.s.l.), Atmos. Chem. Phys., 10, 4583–4596, doi:10.5194/acp-10-4583-2010, 2010.

Engling, G., Zhang, Y.-N., Chan, C.-Y., Sang, X.-F., Lin, M., Ho, K.-F., Li, Y.-S., Lin, C.-Y., and Lee, J. J.: Characterization and sources of aerosol particles over the southeastern tibetan plateau during the southeast asia biomass-burning season, Tellus B, 63, 117–128, doi:10.1111/j.1600-0889.2010.00512.x, 2011.

Farmer, D. K., Matsunaga, A., Docherty, K. S., Surratt, J. D., Seinfeld, J. H., Ziemann, P. J., and Jimenez, J. L.: Response of an aerosol mass spectrometer to organonitrates and organosulfates and implications for atmospheric chemistry, Proc. Natl. Aca. Sci. USA, 107, 6670–6675, doi:10.1073/pnas.0912340107, 2010.

Fierz, M., Vernooij, M. G. C., and Burtscher, H.: An improved low-flow thermodenuder, J. Aerosol. Sci., 38, 1163–1168, doi:10.1016/j.jaerosci.2007.08.006, 2007.

Ge, X., Shaw, S., and Zhang, Q.: Toward understanding amines and their degradation products from post-combustion CO2 capture processes with aerosol mass spectrometry, Environ. Sci. Technol., 48, 5066–5075, doi:10.1021/es4056966, 2014.

Grannas, A. M., Jones, A. E., Dibb, J., Ammann, M., Anastasio, C., Beine, H. J., Bergin, M., Bottenheim, J., Boxe, C. S., Carver, G., Chen, G., Crawford, J. H., Dominé, F., Frey, M. M., Guzmán, M. I., Heard, D. E., Helmig, D., Hoffmann, M. R., Honrath, R. E., Huey, L. G., Hutterli, M., Jacobi, H. W., Klán, P., Lefer, B., McConnell, J., Plane, J., Sander, R., Savarino, J., Shepson, P. B., Simpson, W. R., Sodeau, J. R., von Glasow, R., Weller, R., Wolff, E. W., and Zhu, T.: An overview of snow photochemistry: evidence, mechanisms and impacts, Atmos. Chem. Phys., 7, 4329–4373, doi:10.5194/acp-7-4329-2007, 2007.

Hegde, P. and Kawamura, K.: Seasonal variations of water-soluble organic carbon, dicarboxylic acids, ketocarboxylic acids, and α-dicarbonyls in Central Himalayan aerosols, Atmos. Chem. Phys., 12, 6645–6665, doi:10.5194/acp-12-6645-2012, 2012.

Huffman, J. A., Docherty, K. S., Aiken, A. C., Cubison, M. J., Ulbrich, I. M., DeCarlo, P. F., Sueper, D., Jayne, J. T., Worsnop, D. R., Ziemann, P. J., and Jimenez, J. L.: Chemically-resolved aerosol volatility measurements from two megacity field studies, Atmos. Chem. Phys., 9, 7161–7182, doi:10.5194/acp-9-7161-2009, 2009.

Jimenez, J. L., Canagaratna, M. R., Donahue, N. M., Prevot, A. S. H., Zhang, Q., Kroll, J. H., DeCarlo, P. F., Allan, J. D., Coe, H., Ng, N. L., Aiken, A. C., Docherty, K. S., Ulbrich, I. M., Grieshop, A. P., Robinson, A. L., Duplissy, J., Smith, J. D., Wilson, K. R., Lanz, V. A., Hueglin, C., Sun, Y. L., Tian, J., Laaksonen, A., Raatikainen, T., Rautiainen, J., Vaattovaara, P., Ehn, M., Kulmala, M., Tomlinson, J. M., Collins, D. R., Cubison, M. J., E., Dunlea, J., Huffman, J. A., Onasch, T. B., Alfarra, M. R., Williams, P. I., Bower, K., Kondo, Y., Schneider, J., Drewnick, F., Borrmann, S., Weimer, S., Demerjian, K., Salcedo, D., Cottrell, L., Griffin, R., Takami, A., Miyoshi, T., Hatakeyama, S., Shimono, A., Sun, J. Y., Zhang, Y. M., Dzepina, K., Kimmel, J. R., Sueper, D., Jayne, J. T., Herndon, S. C., Trimborn, A. M., Williams, L. R., Wood, E. C., Middlebrook, A. M., Kolb, C. E., Baltensperger, U., and Worsnop, D. R.: Evolution of organic aerosols in the atmosphere, Science, 326, 1525–1529, doi:10.1126/science.1180353, 2009.

Kanakidou, M., Seinfeld, J. H., Pandis, S. N., Barnes, I., Dentener, F. J., Facchini, M. C., Van Dingenen, R., Ervens, B., Nenes, A., Nielsen, C. J., Swietlicki, E., Putaud, J. P., Balkanski, Y., Fuzzi, S., Horth, J., Moortgat, G. K., Winterhalter, R., Myhre, C. E. L., Tsigaridis, K., Vignati, E., Stephanou, E. G., and Wilson, J.: Organic aerosol and global climate modelling: a review, Atmos. Chem. Phys., 5, 1053–1123, doi:10.5194/acp-5-1053-2005, 2005.

Kondo, Y., Miyazaki, Y., Takegawa, N., Miyakawa, T., Weber, R., Jimenez, J., Zhang, Q., and Worsnop, D. R.: Oxygenated and water-soluble organic aerosols in tokyo, J. Geophys. Res., 112, D01203, doi:10.1029/2006JD007056, 2007.

Lee, A. K. Y., Hayden, K. L., Herckes, P., Leaitch, W. R., Liggio, J., Macdonald, A. M., and Abbatt, J. P. D.: Characterization of aerosol and cloud water at a mountain site during wacs 2010: Secondary organic aerosol formation through oxidative cloud processing, Atmos. Chem. Phys., 12, 7103–7116, doi:10.5194/acp-12-7103-2012, 2012.

Li, J. J., Wang, G. H., Wang, X. M., Cao, J. J., Sun, T., Cheng, C. L., Meng, J. J., Hu, T. F., and Liu, S. X.: Abundance, composition and source of atmospheric pm2.5 at a remote site in the tibetan plateau, china, Tellus B, 65, 1–16, doi:10.3402/tellusb.v65i0.20281, 2013.

Li, S.-M., Tang, J., Xue, H., and Toom-Sauntry, D.: Size distribution and estimated optical properties of carbonate, water soluble organic carbon, and sulfate in aerosols at a remote high altitude site in western china, Geophys. Res. Lett., 27, 1107–1110, doi:10.1029/1999GL010929, 2000.

Li, W. J. and Shao, L. Y.: Observation of nitrate coatings on atmospheric mineral dust particles, Atmos. Chem. Phys., 9, 1863–1871, doi:10.5194/acp-9-1863-2009, 2009.

Meng, J., Wang, G., Li, J., Cheng, C., and Cao, J.: Atmospheric oxalic acid and related secondary organic aerosols in qinghai lake, a continental background site in tibet plateau, Atmos. Environ., 79, 582–589, doi:10.1016/j.atmosenv.2013.07.024, 2013.

Ng, N. L., Canagaratna, M. R., Zhang, Q., Jimenez, J. L., Tian, J., Ulbrich, I. M., Kroll, J. H., Docherty, K. S., Chhabra, P. S., Bahreini, R., Murphy, S. M., Seinfeld, J. H., Hildebrandt, L., Donahue, N. M., DeCarlo, P. F., Lanz, V. A., Prévôt, A. S. H., Dinar, E., Rudich, Y., and Worsnop, D. R.: Organic aerosol components observed in northern hemispheric datasets from aerosol mass spectrometry, Atmos. Chem. Phys., 10, 4625–4641, doi:10.5194/acp-10-4625-2010, 2010.

Pathak, R. K., Wang, T., Ho, K. F., and Lee, S. C.: Characteristics of summertime pm2.5 organic and elemental carbon in four major chinese cities: Implications of high acidity for water-soluble organic carbon (WSOC), Atmos. Environ., 45, 318–325, doi:10.1016/j.atmosenv.2010.10.021, 2011.

Qu, W.-J., Zhang, X.-Y., Arimoto, R., Wang, Y.-Q., Wang, D., Sheng, L.-F., and Fu, G.: Aerosol background at two remote cawnet sites in western china, Sci. Total Environ., 407, 3518–3529, doi:10.1016/j.scitotenv.2009.02.012, 2009.

Ram, K., Sarin, M. M., and Hegde, P.: Atmospheric abundances of primary and secondary carbonaceous species at two high-altitude sites in india: Sources and temporal variability, Atmos. Environ., 42, 6785–6796, doi:10.1016/j.atmosenv.2008.05.031, 2008.

Ram, K., Sarin, M. M., and Hegde, P.: Long-term record of aerosol optical properties and chemical composition from a high-altitude site (manora peak) in central himalaya, Atmos. Chem. Phys., 10, 11791–11803, doi:10.5194/acp-10-11791-2010, 2010.

Rengarajan, R., Sarin, M. M., and Sudheer, A. K.: Carbonaceous and inorganic species in atmospheric aerosols during wintertime over urban and high-altitude sites in north india, J. Geophys. Res., 112, D21307, doi:10.1029/2006jd008150, 2007.

Sang, X., Zhang, Z., Chan, C., and Engling, G.: Source categories and contribution of biomass smoke to organic aerosol over

the southeastern tibetan plateau, Atmos. Environ., 78, 113–123, doi:10.1016/j.atmosenv.2012.12.012, 2013.

Shrestha, P., Barros, A. P., and Khlystov, A.: Chemical composition and aerosol size distribution of the middle mountain range in the nepal himalayas during the 2009 pre-monsoon season, Atmos. Chem. Phys., 10, 11605–11621, doi:10.5194/acp-10-11605-2010, 2010.

Sullivan, R. C., Moore, M. J. K., Petters, M. D., Kreidenweis, S. M., Roberts, G. C., and Prather, K. A.: Timescale for hygroscopic conversion of calcite mineral particles through heterogeneous reaction with nitric acid, Phys. Chem. Chem. Phys., 11, 7826–7837, doi:10.1039/b904217b, 2009.

Sun, Y., Zhang, Q., MacDonald, A. M., Hayden, K., Li, S. M., Liggio, J., Liu, P. S. K., Anlauf, K. G., Leaitch, W. R., Cubison, M., Worsnop, D., van Donkelaar, A., and Martin, R. V.: Size-resolved aerosol chemistry on whistler mountain, canada with a high-resolution aerosol mass spectrometer during intex-b, Atmos. Chem. Phys., 9, 3095–3111, doi:10.5194/acp-9-3095-2009, 2009.

Sun, Y., Zhang, Q., Anastasio, C., and Sun, J.: Insights into secondary organic aerosol formed via aqueous-phase reactions of phenolic compounds based on high resolution aerosol mass spectrometry, Atmospheric Chemistry and Physics, 10, 4809-4822, doi:10.5194/acp-10-4809-2010, 2010.

Sun, Y., Zhang, Q., Zheng, M., Ding, X., Edgerton, E. S., and Wang, X.: Characterization and source apportionment of water-soluble organic matter in atmospheric fine particles (pm2.5) with high-resolution aerosol mass spectrometry and gc–ms, Environ. Sci. Technol., 45, 4854–4861, doi:10.1021/es200162h, 2011.

Takegawa, N., Miyakawa, T., Kawamura, K., and Kondo, Y.: Contribution of selected dicarboxylic and ω-oxocarboxylic acids in ambient aerosol to the m/z 44 signal of an aerodyne aerosol mass spectrometer, Aerosol. Sci. Technol., 41, 418–437, doi:10.1080/02786820701203215, 2007.

Ulbrich, I. M., Canagaratna, M. R., Zhang, Q., Worsnop, D. R., and Jimenez, J. L.: Interpretation of organic components from positive matrix factorization of aerosol mass spectrometric data, Atmos. Chem. Phys., 9, 2891–2918, doi:10.5194/acp-9-2891-2009, 2009.

Wang, G. H., Zhou, B. H., Cheng, C. L., Cao, J. J., Li, J. J., Meng, J. J., Tao, J., Zhang, R. J., and Fu, P. Q.: Impact of Gobi desert dust on aerosol chemistry of Xi'an, inland China during spring 2009: differences in composition and size distribution between the urban ground surface and the mountain atmosphere, Atmos. Chem. Phys., 13, 819–835, doi:10.5194/acp-13-819-2013, 2013.

Wang, Z., Wang, T., Guo, J., Gao, R., Xue, L., Zhang, J., Zhou, Y., Zhou, X., Zhang, Q., and Wang, W.: Formation of secondary organic carbon and cloud impact on carbonaceous aerosols at mount tai, north china, Atmos. Environ., 46, 516–527, doi:10.1016/j.atmosenv.2011.08.019, 2012.

Xu, J., Wang, Z., Yu, G., Sun, W., Qin, X., Ren, J., and Qin, D.: Seasonal and diurnal variations in aerosol concentrations at a high-altitude site on the northern boundary of qinghai-xizang plateau, Atmos. Res., 120–121, 240–248, doi:10.1016/j.atmosres.2012.08.022, 2013a.

Xu, J., Zhang, Q., Li, X., Ge, X., Xiao, C., Ren, J., and Qin, D.: Dissolved organic matter and inorganic ions in a central himalayan glacier–insights into chemical composition and

atmospheric sources, Environ. Sci. Technol., 47, 6181–6188, doi:10.1021/es4009882, 2013b.

Xu, J., Wang, Z., Yu, G., Qin, X., Ren, J., and Qin, D.: Characteristics of water soluble ionic species in fine particles from a high altitude site on the northern boundary of tibetan plateau: Mixture of mineral dust and anthropogenic aerosol, Atmos. Res., 143, 43–56, doi:10.1016/j.atmosres.2014.01.018, 2014a.

Xu, J., Zhang, Q., Chen, M., Ge, X., Ren, J., and Qin, D.: Chemical composition, sources, and processes of urban aerosols during summertime in northwest china: Insights from high resolution aerosol mass spectrometry, Atmos. Chem. Phys., 14, 12593–12611, doi:10.5194/acp-14-12593-2014, 2014b.

Xue, J., Yuan, Z., Lau, A. K. H., and Yu, J. Z.: Insights into factors affecting nitrate in pm2.5 in a polluted high nox environment through hourly observations and size distribution measurements, J. Geophys. Res.-Atmos., 119, 4888–4902, doi:10.1002/2013JD021108, 2014.

Yao, T., Thompson, L. G., Mosbrugger, V., Zhang, F., Ma, Y., Luo, T., Xu, B., Yang, X., Joswiak, D. R., Wang, W., Joswiak, M. E., Devkota, L. P., Tayal, S., Jilani, R., and Fayziev, R.: Third pole environment (tpe), Environ. Dev., 3, 52–64, doi:10.1016/j.envdev.2012.04.002, 2012.

Yu, H. and Yu, J. Z.: Modal characteristics of elemental and organic carbon in an urban location in guangzhou, china, Aerosol. Sci. Technol., 43, 1108–1118, doi:10.1080/02786820903196878, 2009.

Yu, L., Smith, J., Laskin, A., Anastasio, C., Laskin, J., and Zhang, Q.: Chemical characterization of SOA formed from aqueous-phase reactions of phenols with the triplet excited state of carbonyl and hydroxyl radical, Atmos. Chem. Phys., 14, 13801–13816, doi:10.5194/acp-14-13801-2014, 2014.

Zhang, J. K., Sun, Y., Liu, Z. R., Ji, D. S., Hu, B., Liu, Q., and Wang, Y. S.: Characterization of submicron aerosols during a month of serious pollution in Beijing, 2013, Atmos. Chem. Phys., 14, 2887–2903, doi:10.5194/acp-14-2887-2014, 2014a.

Zhang, N., Cao, J., Liu, S., Zhao, Z., Xu, H., and Xiao, S.: Chemical composition and sources of pm2.5 and tsp collected at qinghai lake during summertime, Atmos. Res., 138, 213–222, doi:10.1016/j.atmosres.2013.11.016, 2014b.

Zhang, Q., Alfarra, M. R., Worsnop, D. R., Allan, J. D., Coe, H., Canagaratna, M. R., and Jimenez, J. L.: Deconvolution and quantification of hydrocarbon-like and oxygenated organic aerosols based on aerosol mass spectrometry, Environ. Sci. Technol., 39, 4938–4952, doi:10.1021/es048568l, 2005.

Zhang, Q., Jimenez, J. L., Canagaratna, M. R., Allan, J. D., Coe, H., Ulbrich, I., Alfarra, M. R., Takami, A., Middlebrook, A. M., Sun, Y. L., Dzepina, K., Dunlea, E., Docherty, K., De-Carlo, P. F., Salcedo, D., Onasch, T., Jayne, J. T., Miyoshi, T., Shimono, A., Hatakeyama, S., Takegawa, N., Kondo, Y., Schneider, J., Drewnick, F., Borrmann, S., Weimer, S., Demerjian, K., Williams, P., Bower, K., Bahreini, R., Cottrell, L., Griffin, R. J., Rautiainen, J., Sun, J. Y., Zhang, Y. M., and Worsnop, D. R.: Ubiquity and dominance of oxygenated species in organic aerosols in anthropogenically-influenced northern hemisphere midlatitudes, Geophys. Res. Lett., 34, L13801, doi:10.1029/2007gl029979, 2007.

Zhang, Q., Jimenez, J. L., Canagaratna, M. R., Ulbrich, I. M., Ng, N. L., Worsnop, D. R., and Sun, Y.: Understanding atmospheric organic aerosols via factor analysis of aerosol mass spectrometry: A review, Anal. Bioanal. Chem., 401, 3045–3067, doi:10.1007/s00216-011-5355-y, 2011.

Zhao, Z., Cao, J., Shen, Z., Xu, B., Zhu, C., Chen, L. W. A., Su, X., Liu, S., Han, Y., Wang, G., and Ho, K.: Aerosol particles at a high-altitude site on the southeast tibetan plateau, china: Implications for pollution transport from south asia, J. Geophys. Res., 118, 11360–311375, doi:10.1002/jgrd.50599, 2013.

Zhou, S., Wang, Z., Gao, R., Xue, L., Yuan, C., Wang, T., Gao, X., Wang, X., Nie, W., Xu, Z., Zhang, Q., and Wang, W.: Formation of secondary organic carbon and long-range transport of carbonaceous aerosols at mount heng in south china, Atmos. Environ., 63, 203–212, doi:10.1016/j.atmosenv.2012.09.021, 2012.